JP Journal of Heat and Mass Transfer
Volume 4, Number 1, 2010, Pages 17-39
Published Online: February 25, 2010
This paper is available online at http://www.pphmj.com

EFFECTS OF AN INNER OBJECT ON THE HEAT TRANSFER IN A SIDE-COOLING ENCLOSURE WITH A HEAT SOURCE ON THE OPPOSITE WALL

YUICHI FUNAWATASHI[*], TAKAYUKI KITA and MASARU ISHIZUKA

Department of Mechanical Systems Engineering
Toyama Prefectural University
5180 Kurokawa, Imizu, Toyama 939-0398, Japan
e-mail: fnwtsh@pu-toyama.ac.jp

Abstract

A numerical study has been conducted on the effects of an inner object on the heat transfer in a side-cooling enclosure with a heat source on the opposite wall. It is found that an inner object hinders heat transfer in most of the cases considered in the present study and enhances it by several % in some cases. In the cases where the flow between heat source and object resembles the forced convective flow in a channel with two parallel flat walls, modified Nusselt and modified Grashof numbers for heat transfer correlation are proposed.

Nomenclature

g	gravitational acceleration
$\hat{\mathbf{g}}$	gravity unit vector
Gr	Grashof number
G_1	gap between heat source and inner object

Keywords and phrases: enclosure, inner object, natural convective heat transfer, side cooling, heat transfer correlation, electronic device.

[*]Corresponding author

Received November 16, 2009

G_1^*	dimensionless gap between heat source and inner object
H	height of the enclosure
H_p	height of the inner object
k	thermal conductivity
n	time step
Nu	local Nusselt number
Nu_a	average Nusselt number
Nu_g	modified Nusselt number
p^*	dimensionless pressure
P	scale pressure
Pr	Prandtl number
Re_g	modified Grashof number
T^*	dimensionless temperature
ΔT	scale temperature difference
T_b	bulk temperature
T_b^*	dimensionless bulk temperature
T_c	temperature of the cooling wall
T_h	temperature of the heat source
u_m	average velocity
u_m^*	dimensionless average velocity
$\mathbf{u}^*$	dimensionless velocity vector
U	scale velocity
W	width of the enclosure
W_h	width of the heat source
W_h^*	dimensionless width of the heat source
W_p	width of the inner object
x, y	coordinates
y^*	dimensionless coordinate
$y_1^*, \ y_2^*$	locations of the bottom and top of the heat source

Greek Symbols

α	thermal diffusivity
β	coefficient of thermal expansion
ν	kinematic viscosity
ρ_0	density of fluid
τ	scale time

1. Introduction

Natural convection in enclosures is a major determinant of performance in areas such as solar collectors, heat storage, and cooling of electronic devices. A large number of studies, both numerical and experimental, have been conducted on them, and the fundamental characteristics are now found in the literature [2, 8, 9, 11].

In the field of cooling of electronic devices in enclosures by natural convection, there may be a situation where a heat source is on a vertical side wall, all or a part of the opposite side wall is cooled and the other surface of the wall is adiabatic. Natural convection of this case has already been studied. Nithyadevi et al. [6] studied numerically the effect of the aspect ratio and the locations of a heat source and a cooling part of the wall on the heat transfer. Valencia and Frederick [10] studied numerically the same problem and found that the heat transfer rate is enhanced when the heating location is at the middle of the hot wall.

In electronic component cooling, there usually exist objects around heat sources in an enclosure and these objects can affect the heat transfer, since natural convection is extremely sensitive to the changes in the configuration of enclosures and imposed boundary conditions [9]. This fact means that the natural convective heat transfer in enclosures may be enhanced or hindered by inner objects. Effects of an object in an enclosure on the natural convection heat transfer have been studied by several authors. House et al. [4] have studied numerically the effects of a centered, square conducting body on the natural convection heat transfer in a square enclosure with a temperature difference between side walls. Oh et al. [7] have made a two-dimensional numerical study on the natural convection in a square enclosure with a temperature difference between side walls having a centered square, heat-generating conducting body. Ha and Jung [3] have conducted a three-dimensional numerical analysis on the natural convection in a cubic enclosure in which there is a temperature difference between vertical walls and a cubic heat-generating body is centered.

Although a lot of studies have been conducted on the natural convection in enclosures, to the best of the authors' knowledge, the natural convection in an enclosure with an inner object where a heat source is on a vertical adiabatic side wall, the opposing side wall is fully cooled, and the rest of the wall is adiabatic has not been studied. This type of arrangement of a heat source and a cooling wall is considered one of simplified models of cooling of electronic devices, and a good understanding of its characteristics would be useful in thermal design of electronic systems.

In the present work, two dimensional numerical simulations are conducted to investigate the heat transfer in a square enclosure where a heat source of a constant and uniform temperature is located on the middle of a vertical side wall, the other side wall is kept isothermal at a temperature lower than that of the heat source and the rest of the wall is adiabatic and an adiabatic object is located inside.

Although the model to be considered in the present study may seem too simplified, a deep knowledge of its features is still indispensable to formulate a direction for the best design even in the days when commercial software packages can provide velocity and temperature fields in more complicated cases.

2. Mathematical Formulation and Numerical Procedure

The physical model to be considered is shown in Figure 1. The width and height of the enclosure are designated by W and H, respectively. A heat source of width W_h is set at the center of the side wall, and a rectangular object of width W_p and height H_p is located in the enclosure with a gap G_1. The temperature T_h of the heat source is constant and uniform; the temperature T_c of the opposite side wall is also constant and uniform, with $T_h > T_c$. The rest of the wall is adiabatic. The working fluid is assumed to be air.

The governing equations are the two-dimensional incompressible Navier-Stokes equation, continuity equation, and energy equation. The Boussinesq approximation is enforced; all the fluid properties are assumed to be constant, except density in the buoyancy term.

These equations are given the following non-dimensional forms, where the non-dimensional variables are asterisked:

$$\nabla \cdot \mathbf{u}^* = 0, \tag{1}$$

$$\frac{\partial}{\partial t^*}\mathbf{u}^* + \mathbf{u}^* \cdot \nabla \mathbf{u}^* = -\nabla p^* + \frac{1}{\sqrt{\mathrm{Gr}}}\nabla^2 \mathbf{u}^* + T^* \hat{\mathbf{g}}, \tag{2}$$

$$\frac{\partial T^*}{\partial t^*} + \mathbf{u}^* \cdot \nabla T^* = \frac{1}{\mathrm{Pr}\sqrt{\mathrm{Gr}}}\nabla^2 T^*. \tag{3}$$

The enclosure width W is used as the scale length. The scale velocity U, the scale temperature difference ΔT, the scale time τ, and the scale pressure P are, respectively, defined:

$$U = \sqrt{g\beta W \Delta T}, \tag{4}$$

$$\Delta T = T_H - T_C, \tag{5}$$

$$\tau = \frac{H}{U}, \tag{6}$$

$$P = \rho_0 U^2. \tag{7}$$

The Prandtl number Pr and the Grashof number Gr are, respectively, defined:

$$\mathrm{Pr} = \frac{\nu}{\alpha}, \tag{8}$$

$$\mathrm{Gr} = \frac{g\beta W^3 \Delta T}{\nu^2}. \tag{9}$$

By taking divergence of equation (2), the Poisson equation for the pressure is obtained:

$$\nabla^2 p^* = -\nabla \cdot (\mathbf{u}^* \cdot \nabla \mathbf{u}^*) - \frac{\partial D}{\partial t^*} + \frac{1}{\sqrt{\mathrm{Gr}}}\nabla^2 D + \nabla \cdot T^* \hat{\mathbf{g}}, \tag{10}$$

where

$$D \equiv \nabla \cdot \mathbf{u}^*. \tag{11}$$

Following the MAC method, D is retained here to prevent the accumulation of numerical errors. If a velocity field is given at a certain time, the Poisson equation

can be solved to obtain the pressure field, and with these values of pressure substituted, equation (2) can be integrated to give the velocity at next time.

A transformation of co-ordinates is used to unequally distribute grid points in the physical space. The transformation [1] employed is expressed as

$$\xi = 0.5 + 0.5\,\frac{\ln[(\beta + 2x/h - 1)/(\beta - 2x/h + 1)]}{\ln[(\beta + 1)/(\beta - 1)]}, \tag{12}$$

$$\beta = \left(1 - \frac{\delta}{h}\right)^{-1/2}. \tag{13}$$

Equation (12) transforms the physical space $0 \le x \le h$ to the computational one $0 \le \xi \le 1$. The concentration of grid points is controlled by adjusting the value of δ.

After transformation of co-ordinates, equations (2), (3), (10) are discretized using Kawamura's third-order scheme [5] for the convection term, the central-difference scheme for the other spatial derivatives, and the Euler backward scheme for the time derivative. In order to prevent the accumulation of numerical errors, D at the new time level is forced to be zero. In using the Euler backward scheme, the convection term is linearlized as

$$\mathbf{u}^{*n+1} \cdot \nabla \mathbf{u}^{*n+1} \approx \mathbf{u}^{*n} \cdot \nabla \mathbf{u}^{*n+1}, \tag{14}$$

where superscript stands for time level.

A local Nusselt number Nu on the surface of the heat source is obtained as

$$\mathrm{Nu} = \frac{q_w W}{(T_h - T_c)k} = \left.\frac{\partial T^*}{\partial x^*}\right|_{\text{at heating surface}}. \tag{15}$$

The local Nusselt number is integrated over the surface of the heat source to obtain the average Nusselt number Nu_a:

$$\mathrm{Nu}_a = \frac{1}{W_h^*}\int_{y_1^*}^{y_2^*} \mathrm{Nu}\, dy^*. \tag{16}$$

3. Results and Discussion

Computations were made for various dimensions and positions of the inner object with $H/W = 1.0$, $S_1 = S_2$, $W_h/H = 0.3$ and $\mathrm{Gr} \le 200{,}000$. The Prandtl

number is fixed at 0.7. Computations were also made for the case without an inner object.

In order to evaluate the effect of grid point number on computational results, computations for Gr = 200,000, $G_1/W = 0.2$, $W_p/W = 0.1$ and $H_p/W = 0.7$ were made with four different grid point numbers, the result being shown in Table 1. We can see that the average Nusselt number on the surface of the heat source changes by about 1% as the number of grid point is increased by about 3 times, that is, from 10,830 to 30,348. To save computational time, the following computations were performed with the grid point number of 10,830, though when the size of an inner object is changed the number is changed accordingly.

The results obtained in the present study are steady for all the values of the parameters. In the following subsections, the flow pattern and heat transfer characteristics for the case without an object is first described, and then the effect of an inner object is considered.

3.1. Flow pattern, isotherms and Nusselt number for the case without an object

The flow pattern and isotherms for the case without an object is shown in Figure 2. The flow structure for $\mathrm{Gr} = 100{,}000$ and 200,000 comprises a primary clockwise circulating cell occupying the whole cavity and two smaller secondary cells. The similar flow structure is reported by Nithyadevi et al. [6] in the flow in a square cavity with partially active sides obtained numerically. As the Grashof number is increased, the center of the secondary cell moves toward the side wall. For $\mathrm{Gr} = 50{,}000$ and 20,000, there is no secondary cells and the entire space of the enclosure is filled with one cell.

It is seen from Figure 2 that in the core region the isotherms are nearly horizontal for any value of Grashof number. This means that heat is conducted from top to bottom region there. This heat transport will be a disadvantage to the overall heat transfer.

The average Nusselt number on the surface of the heat source is plotted against the Grashof number in Figure 3. By curve fitting it is found that the relation between Nusselt and Grashof numbers is expressed in the form

$$\mathrm{Nu}_a = 0.454\mathrm{Gr}^{0.259}. \tag{17}$$

3.2. Effects of the gap between object and heat source

The flow patterns for different gaps between object and heat source with $H_p/W = 0.7$, $W_p/W = 0.1$ and Gr = 200,000 are shown in Figure 4. The flow pattern comprises a primary clockwise circulating cell with secondary cells as in the case without an object, but the configurations are different and the region occupied by the secondary cells is larger. When the gap is small, the flow between object and heat source is like the forced convective flow in a channel with two parallel flat walls, and a large secondary cell forms in the space on the right of the object, as shown in Figure 4(a). As the gap increases, first a stagnant region and then a circulating flow appears in the space between object and heat source. When the object is at the middle of the enclosure, a cell almost the same size forms at each side of the object. When the object is near the right wall of the enclosure, the left secondary cell becomes larger and the flow in the right space is like the forced convective flow in a channel with two parallel flat walls. These features of flow pattern are common to the flows for the other values of Grashof number.

In the core region of the enclosure the isotherms are almost horizontal, which means that heat is transferred from top to bottom by thermal conduction. Compared with the case without an object, isotherms are concentrated in the space on the left of the object and coarse in the space on the right of the object.

Figure 5 demonstrates the effect of the gap between object and heat source on the heat transfer. The result of the case of no object is also plotted for comparison. It is observed in this figure that at Gr = 200,000, average Nusselt numbers for $G_1/W = 0.2$, 0.3 and 0.45 are almost the same as that for the case of no object, while it is lower for $G_1/W = 0.1$ and 0.8 than for the case of no object. This is partly attributed to the reduction of the flow rate between obstacle and heat source, or between obstacle and cooling wall. At Gr = 50,000 and 100,000, however, for any value of G_1/W considered in this study, the Nusselt number is lower in the case with an object than in the case without an object. It is also found that the object hinders the heat transfer more with lower Grashof numbers than with higher Grashof numbers.

3.3. Effects of the width of an object

The flow patterns and isotherms for different values of the width of the object with $H_p/W = 0.7$, $G_1 = G_2$ and Gr = 200,000 are shown in Figure 6. The flow

structure comprises a primary clockwise circulating cell flowing along the inner wall of the enclosure and a smaller secondary cell at each side of the object. The secondary cell decreases in size as the width increases, and for $W_p/W = 0.7$ and 0.8 secondary cells do not appear, in which case the geometry of the space might be called *square loop*. These features of flow pattern are essentially the same when the value of the Grashof number is changed to 50,000 and 100,000.

It is observed in this figure that the temperature field is quite different from that in the case of no object, especially when the width is larger. The core region, where isotherms are nearly horizontal and parallel in the case of no object, is occupied by the object, and in the spaces over and under the object, the portion where the temperature is almost uniform increases in area with increasing width of the object. It means that the effective parts of the heat source and cooling wall decrease in area with increasing width of the object.

Figure 7 demonstrates the effect of the width of the object on heat transfer. It is found in this figure that the Nusselt number decreases with increasing width of the object. The degree of the decrease becomes larger as the Grashof number becomes lower or as the width becomes larger.

3.4. Effects of the height of an object

The flow patterns for different values of the height of the object with $G_1/W = 0.2$, $W_p/W = 0.1$ and $\mathrm{Gr} = 200{,}000$ are shown in Figure 8. The flow structure comprises a primary clockwise circulating cell flowing along the inner wall of the cavity and a secondary cell in the space on the right of the object. The flow in the space between object and heat source can be regarded the forced convective flow in a channel with two parallel flat walls with a portion of low velocity, which increases in size with increasing height of the object. The size of the secondary cell on the right of the object also increases with increasing height of the object.

It is observed that even a small object can disturb the temperature field significantly.

In Figure 9 is shown the effect of the height on heat transfer. In contrast to the effects of the position and the width of the obstacle, it is observed in this figure that at certain values of the height of the object heat transfer can be enhanced. Nusselt numbers for $H_p/W = 0.1, 0.2, 0.4, 0.6$ are higher than in the case of no obstacle.

For $H_p/W = 0.8$, the heat transfer is hindered by the object, and the degree of the decrease of the Nusselt number increases as the Grashof number decreases.

4. Heat Transfer Correlation

The relation between Nusselt and Grashof numbers is considerably affected by the presence of an inner object, as described in the previous sections. In this section, new variables for a correlation of the heat transfer covering a wide range of parameters are proposed.

In the forced convective flow in a channel with two parallel flat walls, the Nusselt number is dependent on the Reynolds number, Prandtl number, and boundary conditions, where the reference velocity and length are, for example, the average velocity and the gap between the plates, respectively.

In some cases of the present study, the flow patterns in the space between object and heat source resemble the forced convective flow in a channel with two parallel flat walls. In such cases if we take the average velocity u_m in the space between heat source and object and the bulk temperature T_b in the cross section at the entrance into this space as reference velocity and reference temperature, respectively, and define Nusselt number Nu_g and Reynolds number Re_g as

$$\mathrm{Nu}_g = \frac{q_w G_1}{(T_h - T_b)k} \tag{18}$$

and

$$\mathrm{Re}_g = \frac{u_m G_1}{\nu}, \tag{19}$$

respectively, then Nu_g can be expressed as a function of Re_g and Pr:

$$\mathrm{Nu}_g = f(\mathrm{Re}_g, \mathrm{Pr}). \tag{20}$$

By using the dimensionless variables, Nu_g and Re_g can be expressed as

$$\mathrm{Nu}_g = \frac{\mathrm{Nu}_a G_1^*}{1 - T_b^*} \tag{21}$$

and

$$\mathrm{Re}_g = \mathrm{Gr}^{1/2} u_m^* G_1^*, \tag{22}$$

respectively, where

$$G_1^* = \frac{G_1}{W}, \tag{23}$$

$$T_b^* = \frac{T_b - T_c}{T_h - T_c}, \tag{24}$$

$$u_m^* = \frac{u_m}{U}. \tag{25}$$

Substituting equations (21) and (22) into equation (20), we can find a relation between Nu_a and Gr. Hereafter we will refer to Nu_g as modified Nusselt number and Re_g as modified Grashof number.

The relation between Nu_g and Re_g for the present result is shown in Figure 10, T_b^* being evaluated in the vertical section through the bottom left corner of the object. The plotted data are categorized into three groups A, B, and C according to flow patterns in the space between object and heat source. Typical examples of these flow patterns are shown in Figure 11. Group A contains the data for the flow pattern resembling the forced convective flow in a channel with two parallel flat walls (Figure 11(a)), group B contains the data for the flow pattern resembling the forced convective flow in a channel with two parallel flat walls but having a small circulating cell within itself (Figure 11(b)), and group C contains the data for the other types of flow pattern (Figure 11(c)). Figure 11 reveals that the data in group A are well correlated by using modified Nusselt and modified Grashof numbers.

A careful examination of the relation between modified Nusselt and modified Grashof numbers in group A reveals that the increasing rate of the modified Nusselt number with the modified Grashof number is affected by the size of the gap. Taking this into account, we can obtain a more accurate correlation

$$\frac{\mathrm{Nu}_a G_1^*}{1 - T_b^*} = a(\mathrm{Gr}^{1/2} u_m^* G_1^*)^b, \tag{26}$$

where

$$a = 14.3G_1^{*2} - 0.712G_1^{*} + 0.221, \tag{27}$$

$$b = -19.6G_1^{*2} + 3.81G_1^{*} + 0.654. \tag{28}$$

In Figure 12, the proposed correlation in equation (26) and the employed numerical data are shown. A good agreement between the equation and the numerical data is observed.

The fact that the heat transfer is well correlated by the modified Nusselt and modified Grashof numbers means that the heat transfer is dominated by both the bulk temperature of the fluid at the entrance to the space between object and heat source and the average flow rate there if the flow resembles the forced convective flow in a channel with two parallel flat walls without regard to the position and size of the object. Therefore, the last task for the complete prediction of the heat transfer is to relate the bulk temperature and flow rate to the position and size of the object. This task is left to a future study.

5. Conclusion

Numerical study was conducted on natural convective heat transfer in a square enclosure where a heat source of a constant and uniform temperature is located on the middle of a vertical side wall, the other side wall is kept isothermal at a temperature lower than that of the heat source and the rest of the wall is adiabatic and an adiabatic object is located inside. The key findings of the study are as follows:

1. In the case without an inner object, flow patterns are classified into two types: flow pattern comprising a circulating cell occupying the whole space for lower Grashof numbers, and flow pattern comprising a primary circulating cell occupying the whole space and two smaller secondary cells for higher Grashof numbers.

2. In most of the cases considered in the present study, heat transfer is hindered by the existence of an inner object, and only in the several cases heat transfer is enhanced by several percent.

3. In the cases with an inner object, flow patterns in the space between the heat source and the inner object are classified into three types: (1) flow pattern resembling the forced convective flow in a channel with two parallel flat walls, (2) flow pattern resembling the forced convective flow in a channel with two parallel flat walls but having a small circulating cell, and (3) the other types.

4. When a flow pattern in the space between heat source and inner object resembles the forced convective flow in a channel with two parallel flat walls, heat transfer characteristics are well correlated by the modified Nusselt and modified Grashof numbers proposed in the present study.

References

[1] D. A. Anderson, J. C. Tannehill and R. H. Pletcher, Computational Fluid Mechanics and Heat Transfer, pp. 247-252, Hemisphere, Washington D.C., 1984.

[2] B. Gebhart, Y. Jaluria, R. L. Mahajan and B. Sammakia, Buoyancy-induced Flows and Transport, pp. 725-814, Hemisphere, Washington D.C., 1988.

[3] M. Y. Ha and M. J. Jung, A numerical study on three-dimensional conjugate heat transfer of natural convection and conduction in a differentially heated cubic enclosure with a heat-generating cubic conducting body, Int. J. Heat Mass Transfer 43 (2000), 4229-4248.

[4] J. M. House, C. Beckermann and T. F. Smith, Effect of a centered conducting body on natural convection heat transfer in an enclosure, Numerical Heat Transfer Part A 18 (1990), 213-225.

[5] T. Kawamura and K. Kuwahara, Computation of high Reynolds number flow around a circular cylinder with surface roughness, AIAA 22nd Aerospace Sciences Meeting, AIAA-84-0340, 1984.

[6] N. Nithyadevi, P. Kandaswamy and J. Lee, Natural convection in a rectangular cavity with partially active side walls, Int. J. Heat Mass Transfer 50 (2007), 4688-4697.

[7] J. Y. Oh, M. Y. Ha and K. C. Kim, Numerical study of heat transfer and flow of natural convection in an enclosure with a heat-generating conducting body, Numerical Heat Transfer Part A 31 (1997), 289-303.

[8] S. Ostrach, Natural convection heat transfer in cavities and cells, Proc. 7th Int. Heat Transfer Conf. 1 (1982), 365-379.

[9] S. Ostrach, Natural convection in enclosures, J. Heat Transfer 110 (1988), 1175-1190.

[10] A. Valencia and R. L. Frederick, Heat transfer in square cavities with partially active vertical walls, Int. J. Heat Mass Transfer 32 (1989), 1567-1574.

[11] R. O. Warrington, Jr. and R. E. Powe, The transfer of heat by natural convection between bodies and their enclosures, Int. J. Heat Mass Transfer 28 (1985), 319-330.

Table 1. Grid point number dependency of Nusselt number

Grid point number	Average Nusselt number on the heat source
3420	10.94
10830	10.73
21105	10.65
30348	10.62

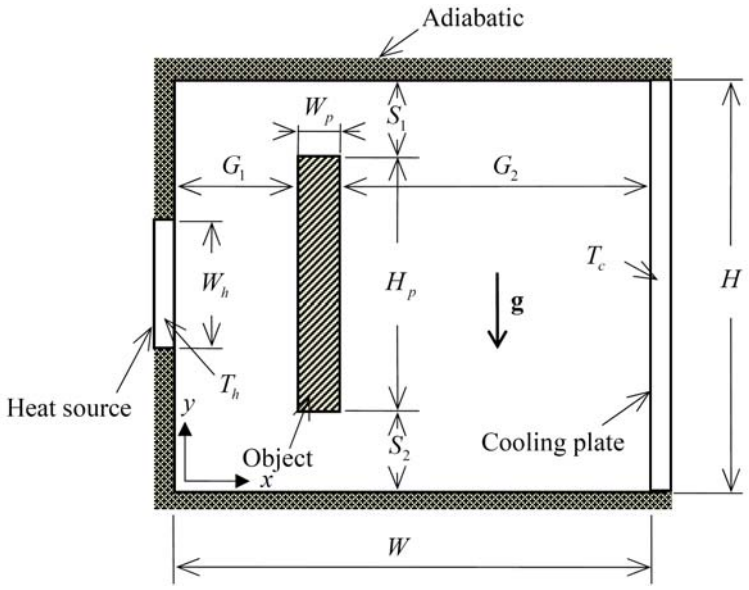

Figure 1. Physical model.

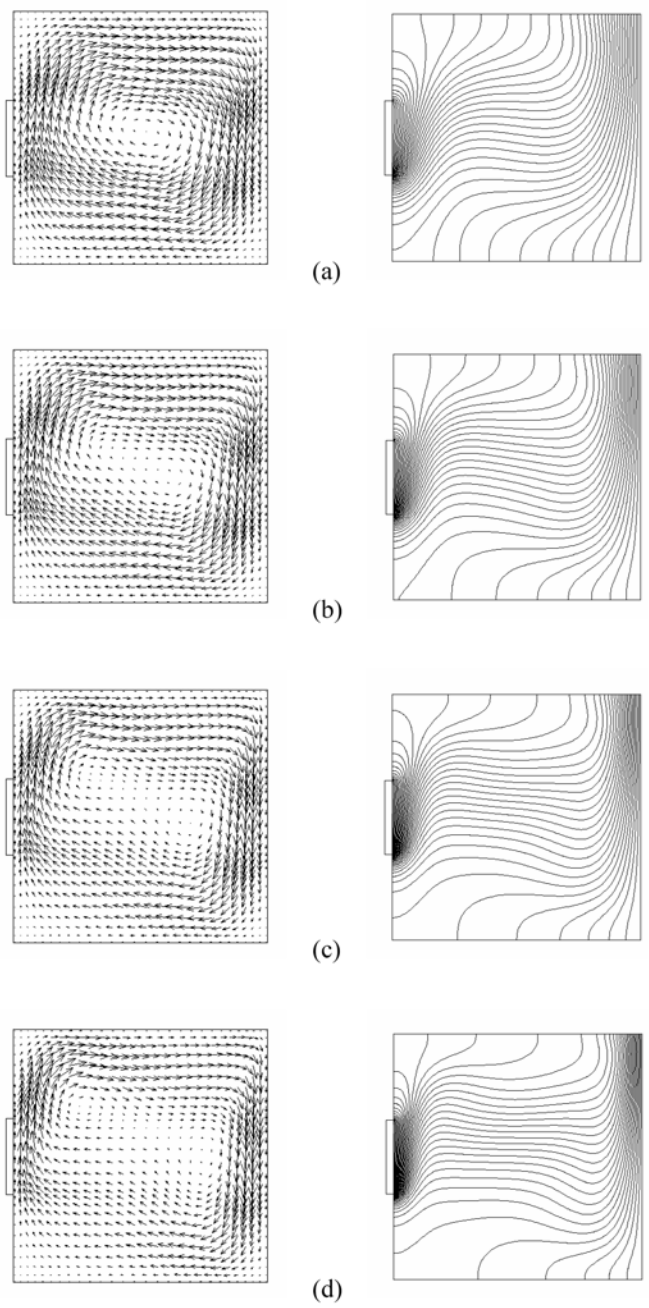

Figure 2. Flow pattern (left) and isotherms for the case without an object: (a) Gr = 20,000; (b) Gr = 50,000; (c) Gr = 100,000; (d) Gr = 200,000.

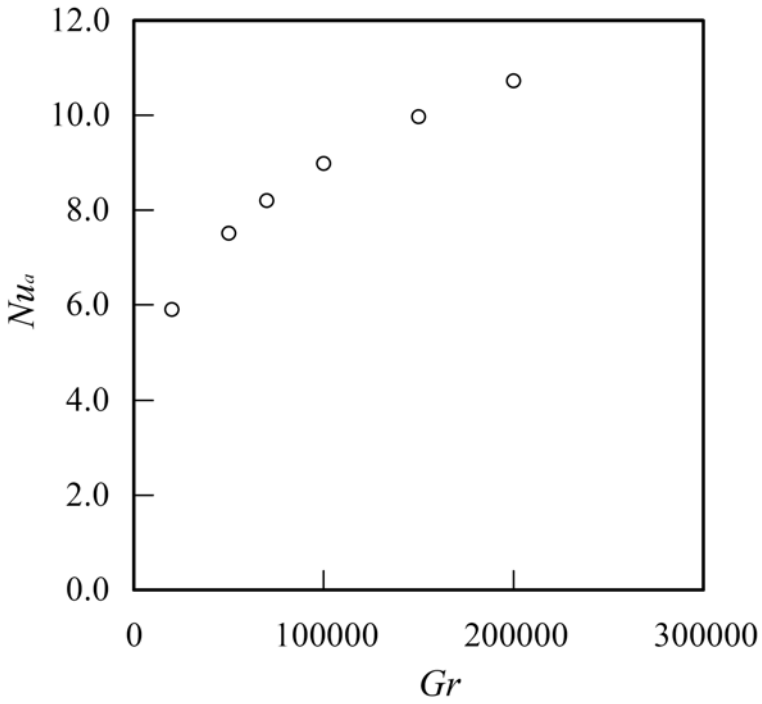

Figure 3. Nusselt number for the case without an object.

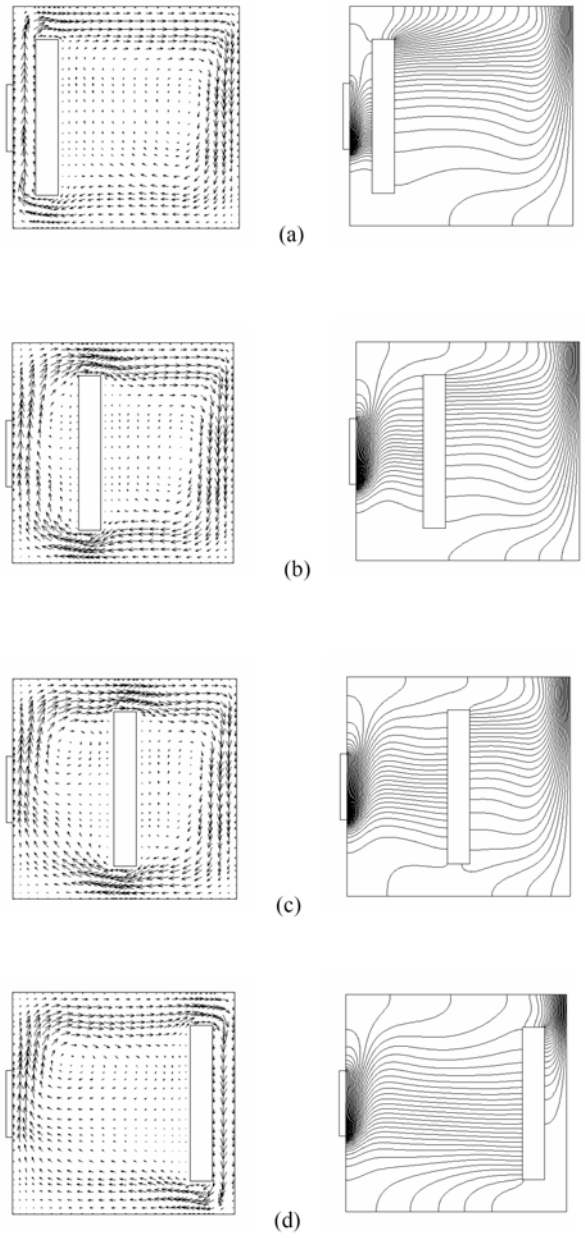

Figure 4. Effect of the gap on the flow (left) and temperature fields for $H_p/W = 0.7$, $W_p/W = 0.1$ and Gr = 200,000 : (a) $G_1/W = 0.1$; (b) $G_1/W = 0.3$; (c) $G_1/W = 0.45$; (d) $G_1/W = 0.8$.

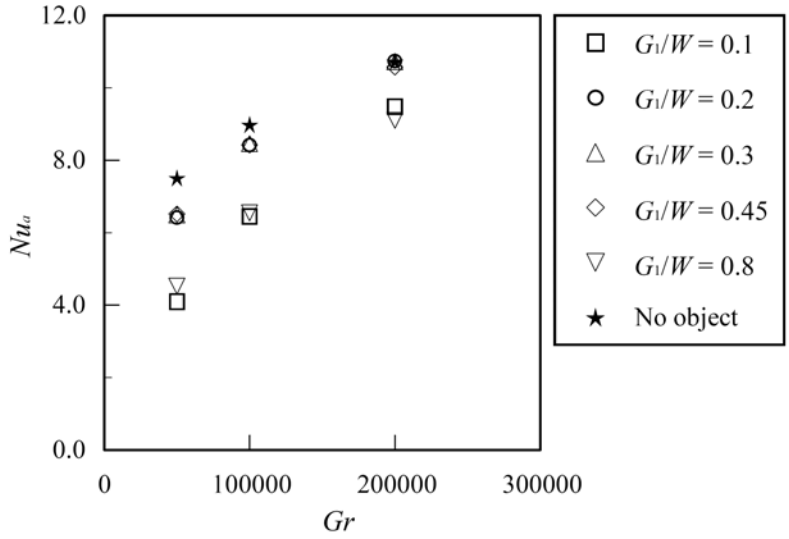

Figure 5. Effect of the gap between object and heat source on the heat transfer for $H_p/W = 0.7,\ W_p/W = 0.1$.

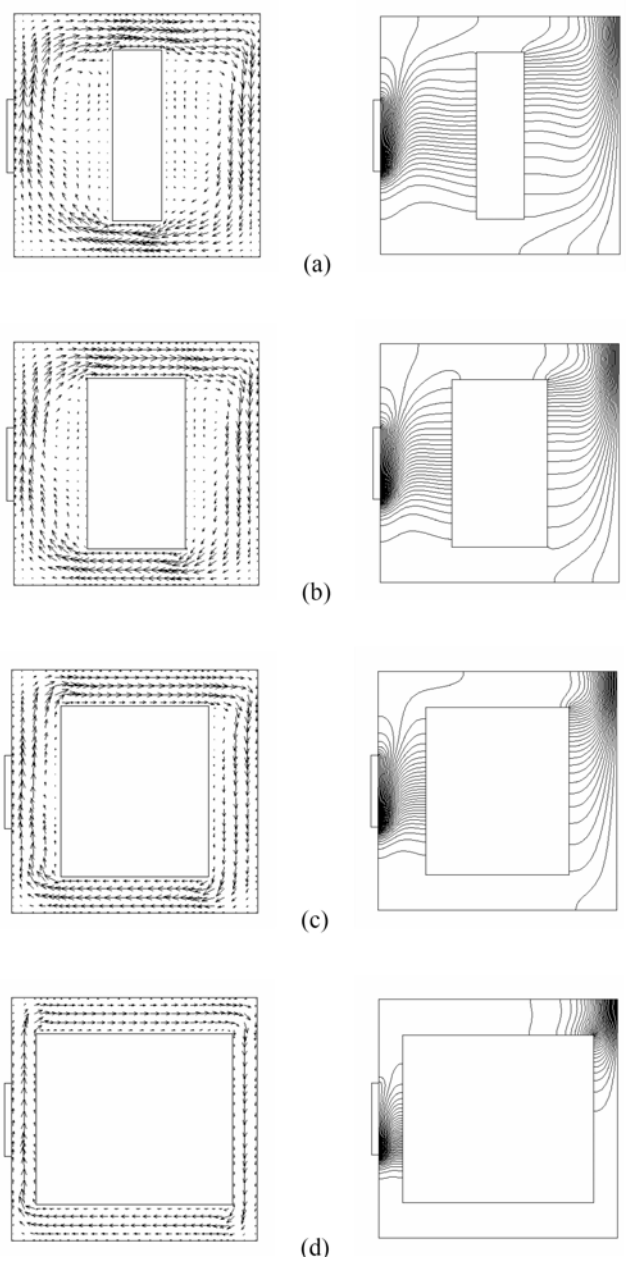

Figure 6. Effect of the width of an object on the flow (left) and temperature fields for $H_p/W = 0.7$, $G_1 = G_2$ and Gr = 200,000 : (a) $W_p/W = 0.2$; (b) $W_p/W = 0.4$; (c) $W_p/W = 0.6$; (d) $W_p/W = 0.8$.

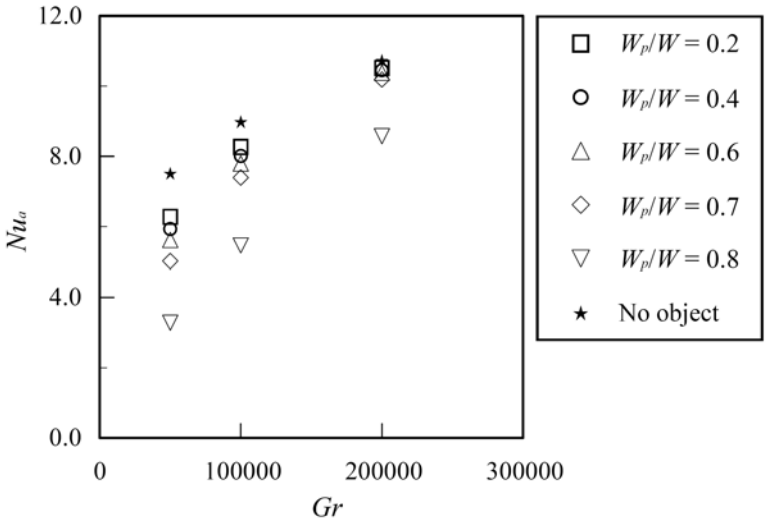

Figure 7. Effect of the width of an object on the heat transfer for $H_p/W = 0.7$.

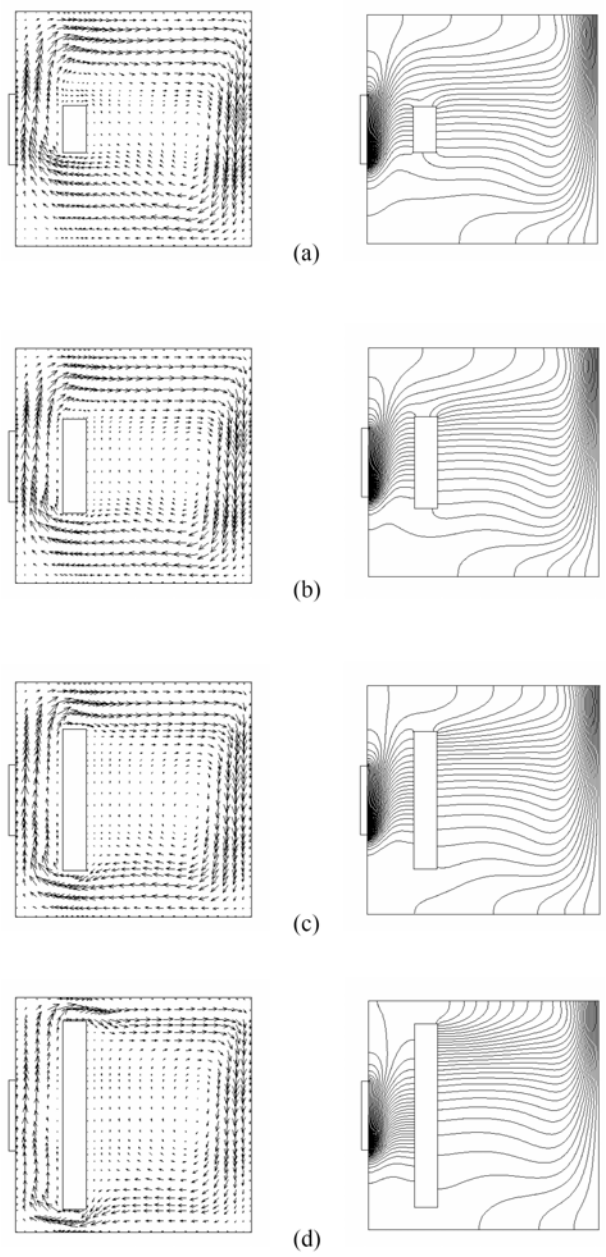

Figure 8. Effect of the height of an object on the flow (left) and temperature fields for $G_1/W = 0.2$, $W_p/W = 0.1$ and Gr = 200,000 : (a) $H_p/W = 0.2$; (b) $H_p/W = 0.4$; (c) $H_p/W = 0.6$; (d) $H_p/W = 0.8$.

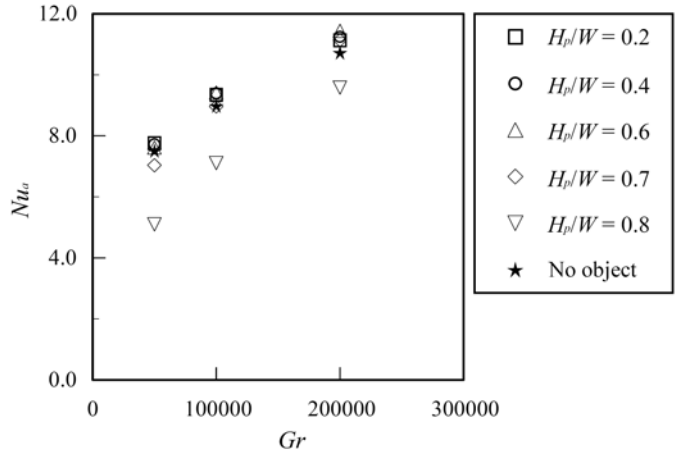

Figure 9. Effect of the height of an object on the heat transfer $G_1/W = 0.2$, $W_p/W = 0.1$.

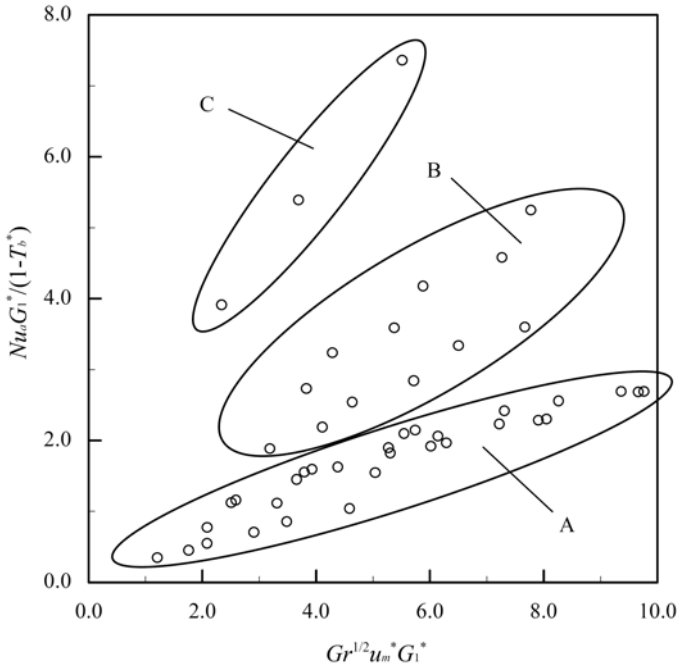

Figure 10. Relation between modified Nusselt and modified Grashof numbers.

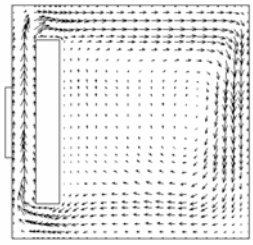

(a)

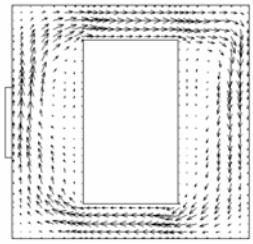

(b)

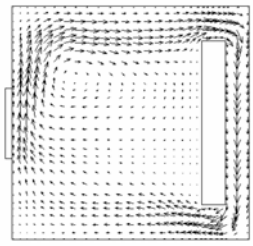

(c)

Figure 11. Three types of flow pattern.

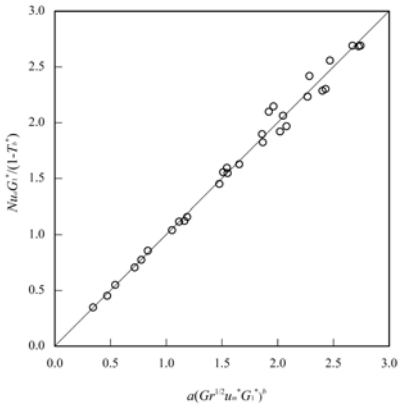

Figure 12. Heat transfer correlation.